Radial distributions of charged-particle densities and electric field strength in the positive column

A. Metze,* D. W. Ernie, and H. J. Oskam

Department of Electrical Engineering, University of Minnesota, Minneapolis, Minnesota 55455

(Received 28 October 1988)

A model is presented for the radial distribution of ion and electron densities and electric field strength in the positive column of a dc discharge for a plasma consisting of a singly charged positive-ion species, electrons, and neutral species. The set of equations involved consists of the particle- and momentum-conservation equations for the ions and electrons and Poisson's equation. Utilizing this single set of equations and appropriate assumptions, the model has been solved, through suitable numerical techniques, for various gas pressures p_0 and tube radii R. These calculations show the development of both the electric field in the "bulk" of the positive column and the sheath field "near" the discharge wall. The results also demonstrate the existence of a nonzero difference between the ion and electron densities at the discharge axis, with an increase in this difference for decreasing $p_0 R$. The importance of including the various terms in the momentum-conservation equations of both the ions and electrons when solving the model has been investigated. The model can be used to calculate the radial properties of positive-column discharges for conditions ranging from the ambipolar diffusion limit to the free-diffusion limit.

I. INTRODUCTION

Several authors have reported theories concerning the radial distributions of charged-particle densities and the electric field strength in the cylindrical positive column of a direct-current discharge. These theories were all confined to plasmas containing a singly charged positive-ion species and electrons, with the authors making various assumptions in order to arrive at an analytic or, more recently, a numerical solution. The set of equations used in these theories consists of the continuity and conservation of momentum equations of the charged particles. To obtain a self-consistent solution, the electric field strength needed in the conservation of momentum equations must be calculated using Poisson's equation. The various approximations reported in the literature involve the assumption of quasineutrality of the plasma, i.e., the electron density $n_e(\mathbf{r})$ is equal to the ion density $n_i(\mathbf{r})$, and the neglect of certain terms in the conservation of momentum equations.

Schottky[1] developed an ambipolar diffusion theory in 1924 in which he assumed quasineutrality of the plasma and neglected the effect of charged-particle inertia on the radial structure of the positive column. Subsequent authors have also assumed quasineutrality of the plasma, but included the charged-particle inertia term in the conservation of momentum equations.[2,3] Several other authors included Poisson's equation for calculating the radial electric field strength inside the plasma.[4–8] However, in order to arrive at a tractable solution, they either omitted the charged-particle inertia term[4–6] or the effect of ion density diffusion on the ion current density towards the discharge walls.[7,8] All the authors have assumed a Maxwellian distribution of the random energy of the ions and electrons with constant ion and electron temperatures.

This paper deals with calculations of the radial charged-particle density distributions, the radial charged-particle current densities, and the radial electric field strength in the cylindrical positive column of a dc discharge. The set of equations involved consists of the particle-conservation equations, the momentum-conservation equations including the diffusion, the electric field force, and the inertia terms, and Poisson's equation. The common assumption that the energy distribution of the random energies of the electrons and ions is Maxwellian with temperatures independent of radial position will be made. In the next section the assumptions used in deriving the model and the resulting set of equations will be given, along with the method of solution used in the numerical calculations. The results obtained for realistic discharge parameters and for various values of the discharge gas pressure p_0 and tube radius R will be presented and discussed in Sec. III. The validity of the assumptions used will be compared with the calculated results in order to determine the self-consistency of the theory presented. Finally, the relative importance of the various terms in the conservation of momentum equations of the ions and electrons on the total radial charged-particle flow density will be discussed in Sec. IV.

II. THEORETICAL MODEL

In the first part of this section, the assumptions used in deriving the model will be discussed. The resulting equations used for the calculations of the radial distributions of the charged-particle densities and the electric field strength will then be presented. Finally, the boundary conditions for the model and the method of solution of the set of equations will be given in the last two parts of this section.

4117

A. Assumptions

The model and calculations presented in this paper refer to a positive column of a dc gaseous discharge with cylindrical symmetry. The plasma is assumed to consist of a singly charged positive-ion species, electrons, and neutral species. The following assumptions will be made for the present model.

(1) The energy distribution of the random energy of the ions and electrons is Maxwellian with temperatures T_i and T_e, respectively. This is an assumption made by all previous authors.

(2) All quantities are independent of the axial coordinate z and the azimuthal angle ϕ.

(3) The ion and electron temperatures T_i and T_e are independent of the radial coordinate r. This assumption was also made by all previous authors.

(4) The ionization frequency ν_i of the electrons is very small with respect to the collision frequencies for momentum transfer ν_{mi} and ν_{me} of the ions and electrons, respectively. Therefore the effect of ionizing collisions on the momentum loss (gain) of the charged particles can be neglected.

(5) The ion and electron production is a linear function of the electron density, while the only charged-particle loss from the plasma is by diffusion towards the discharge tube wall. The calculations can be extended to nonlinear production (loss) processes. However, the main features of the results presented would not change significantly.

(6) The friction force between the ions and electrons can be neglected with respect to the friction force between the charged particles and the neutral particles. This is a valid assumption for low degrees of ionization.

(7) The positive column is in steady state with no net current flowing to the discharge tube wall, so that the radial ion and electron particle flow densities are equal.

B. Equations

The assumptions given above result in the following set of equations:

$$\frac{1}{r}\frac{d}{dr}[r\Gamma_r(r)]=\nu_i n_e(r) \ , \tag{1}$$

$$\frac{m_i}{r}\frac{d}{dr}\left[\frac{r\Gamma_r^2(r)}{n_i(r)}\right]+kT_i\frac{d}{dr}n_i(r)-en_i(r)E_r(r)$$
$$=-m_i\Gamma_r(r)\nu_{mi} \ , \tag{2}$$

$$\frac{m_e}{r}\frac{d}{dr}\left[\frac{r\Gamma_r^2(r)}{n_e(r)}\right]+kT_e\frac{d}{dr}n_e(r)+en_e(r)E_r(r)$$
$$=-m_e\Gamma_r(r)\nu_{me} \ , \tag{3}$$

$$\frac{1}{r}\frac{d}{dr}[rE_r(r)]=\frac{e}{\epsilon_0}[n_i(r)-n_e(r)] \ . \tag{4}$$

Here, $\Gamma_r(r)$ is the radial particle flow density of the ions and electrons; $n_i(r)$ and $n_e(r)$ are the ion and electron particle densities; m_i and m_e are the ion and electron masses; ϵ_0 is the permittivity of free space; and $E_r(r)$ is the radial component of the electric field strength.

Equation (1) is the continuity equation of the charged particles, while Eqs. (2) and (3) are the conservation of momentum equations (volume force equations) for the ions and electrons, respectively. Equation (4) is Poisson's equation and is needed for a self-consistent calculation of the radial electric field strength. The assumption that the ion and electron temperatures are independent of coordinates eliminates the need to use the conservation of energy equations for the ions and the electrons.

The term on the right-hand side of Eqs. (2) and (3) is the friction volume force. Since the radial drift velocity of the neutral particles is very small with respect to the radial drift velocities of the ions and electrons, it is neglected in this term. The terms on the left-hand side of Eqs. (2) and (3) are the inertia volume force, the diffusion volume force, and the electric field volume force, respectively. Previous theories of the radial properties of the positive column which incorporated Poisson's equation have used various approximations concerning the effect of the different volume force terms on the radial particle density distributions, etc. Several authors have neglected one or both inertia volume force terms,[4-7] while two authors neglected the diffusion volume force for the ions.[7,8] The motivation for these approximations results from the fact that when all three volume force terms on the left-hand side of Eq. (2) are included in the theoretical model, an instability occurs in the numerical calculations (for certain numerical techniques) when the radial ion drift energy is equal to one half the kinetic ion pressure, i.e., the radial ion drift velocity v_{di} is equal to the isothermal ion sound speed $v_{si}=(kT_i/m_i)^{1/2}$. This instability problem in the numerical techniques has been discussed in the literature.[8-10] The method described below for solving the set of Eqs. (1)–(4) circumvents this difficulty.

C. Boundary conditions

The four functions to be determined from Eqs. (1)–(4) are $n_i(r)$, $n_e(r)$, $\Gamma_r(r)$, and $E_r(r)$. Appropriate boundary conditions are thus required for these functions. Because of symmetry, both $\Gamma_r(r)$ and $E_r(r)$ must be zero at the axis of the positive column, i.e., $\Gamma_r(r=0)=0$ and $E_r(r=0)=0$. The two other required boundary conditions are the values of $n_i(r=0)$ and $n_e(r=0)$. For the model presented here, these values will be different, i.e., $n_i(r)\neq n_e(r)$, since it will not be assumed that the discharge plasma is quasineutral. It should be noted that the values of $n_i(r=0)$ and $n_e(r=0)$ then determine the spatial derivative of $E_r(r)$ at $r=0$. Moreover, the cylindrical symmetry of the positive column requires that the radial derivatives of $n_i(r)$ and $n_e(r)$ are equal to zero at $r=0$.

The boundary condition for the electron density at the wall of the discharge tube has been discussed by several authors. A summary of this discussion is given in Ingold.[8] If it is assumed that the velocity distribution of the electrons at the wall, which is assumed to be a perfect sink for the electrons, is Maxwellian in the forward direction and zero in the backward direction, then the following boundary condition must hold at the wall:

$$n_e(R) = \Gamma_r(R) \left[\frac{2kT_e}{\pi m_e} \right]^{-1/2} . \qquad (5)$$

This condition is also the boundary condition resulting from collisionless space-charge theory and is equal or very close to the boundary condition of other theories.

D. Method of solution

The method of solution used in this paper consists of expanding the functions $n_i(r)$, $n_e(r)$, $\Gamma_r(r)$, and $E_r(r)$ in power series of the radial coordinate r, around $r = 0$. The calculation of the coefficients of the four power series is performed in the following steps.

(1) The boundary conditions $\Gamma_r(r = 0) = 0$ and $E_r(r = 0) = 0$ as well as the symmetry conditions (i.e., the radial derivatives of the charged-particle densities equal zero at $r = 0$) are used. The values of $n_i(r = 0)$, $n_e(r = 0)$, and the constants v_i, v_{mi}, v_{me}, T_i, and T_e are chosen and substituted into Eqs. (1)–(3). These values will depend on the parameters of the experimental situation being modeled, such as the electric current density inside the positive column, the type of gas, the gas pressure, the tube radius, etc., and can be appropriately chosen. For example, the collision frequencies and charged-particle temperatures may be available from experimental data presented in the literature or can be theoretically calculated.

(2) The coefficients of the power series are determined, either by a standard computer technique or, if possible, by deriving a recurrence relation between the coefficients. During the calculations, nonphysical solutions for the unknown functions may occur. As a result, one of the parameters, e.g., v_i, is changed until a physical solution having sufficient accuracy is obtained. The accuracy can be determined by extending the power series to higher powers of r and comparing the results.

(3) The radius of the discharge tube wall is determined from Eq. (5). If the calculated tube radius is different from the desired tube radius, the calculations are repeated using a different value for the net charged-particle density at the axis $\Delta n(r = 0) = n_i(r = 0) - n_e(r = 0)$. The calculations are repeated until the proper consistency is reached between the tube radius for the experimental conditions being modeled and the theoretical results.

It should be noted that the set of Eqs. (1)–(4) can easily be transformed into a set of dimensionless equations, with the same method of solution being used to obtain the dependence of positive-column properties on discharge parameters. Most previous authors have used the dimensionless approach when developing theories concerning the positive column. However, since the present paper attempts to model the properties of positive-column discharges for which experimental information is available, the dimensionless approach has been avoided.

III. NUMERICAL CALCULATIONS AND DISCUSSION

Numerical calculations were performed for the model presented in Sec. II, utilizing the method of solution out-

lined. These calculations were for a discharge in helium with the following assumed parameters: $m_i = 4$ amu (for He^+), $v_{mi}/p_0 = 3.0 \times 10^7$ s^{-1}Torr^{-1} (for He^+), $v_{me}/p_0 = 2.3 \times 10^9$ s^{-1}Torr^{-1}, $T_i = 300$ K, and $n_i(r = 0) = 1.0 \times 10^{16}$ m^{-3}, where the values for v_{mi} and v_{me} are from Ref. 11. Results are presented below for different values of p_0 and R. For each selection of p_0 and R, the appropriate value for T_e was chosen from the experimental work of Leiby and Rogers[12] and the values of v_i and $n_e(r = 0)$ were adjusted, as indicated in Sec. II, to give a physical solution consistent with the chosen values of p_0 and R.

Figures 1–3 show the results of calculations for a discharge gas pressure $p_0 = 5$ Torr and a tube radius $R = 1.0$ cm, leading to the product $p_0R = 5.0$ Torr cm. From the results of Leiby and Rogers, these conditions imply an electron temperature $T_e = 26\,000$ K. The required net charged-particle density on the axis is then $\Delta n(r = 0) = 6.8 \times 10^{12}$ m^{-3}, with an ionization collision frequency $v_i = 1.95 \times 10^4$ s^{-1}. Figure 1 gives the plots of the ion density $n_i(r)$, the electron density $n_e(r)$, and the net charged-particle density $\Delta n(r)$. The curves for $n_i(r)$ and $n_e(r)$ are close to the shape of the zero-order Bessel function $J_0(2.4r/R)$ resulting from the ambipolar diffusion theory for the positive column.[13] However, there is a deviation from this shape, especially for $n_i(r)$, near the tube wall. This deviation is indicative of the development of a thin sheath region near the wall, which is not modeled by the ambipolar theory. The development of this sheath region is also indicated in the curve of $\Delta n(r)$, which increases rapidly near the wall. From these results it can be seen that, while this model predicts the development of a sheath region, there is no clear distinction between the sheath region and the bulk plasma, as can be expected. Therefore, the assignment of different regions of the discharge to these two categories is somewhat arbitrary, as discussed previously by Self and
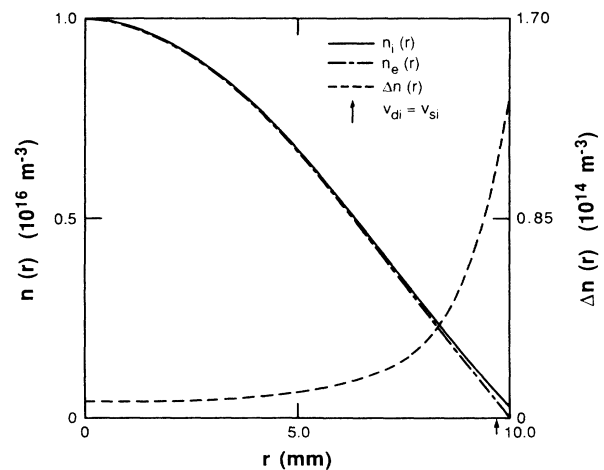

FIG. 1. Numerical calculations of the radial distributions for the ion density $n_i(r)$, the electron density $n_e(r)$, and the net charged-particle density $\Delta n(r)$ in a helium discharge with $p_0 = 5.0$ Torr and $R = 1.0$ cm ($p_0R = 5.0$ Torr cm), implying $T_e = 26\,000$ K, and yielding $v_i = 1.95 \times 10^4$ s^{-1}.
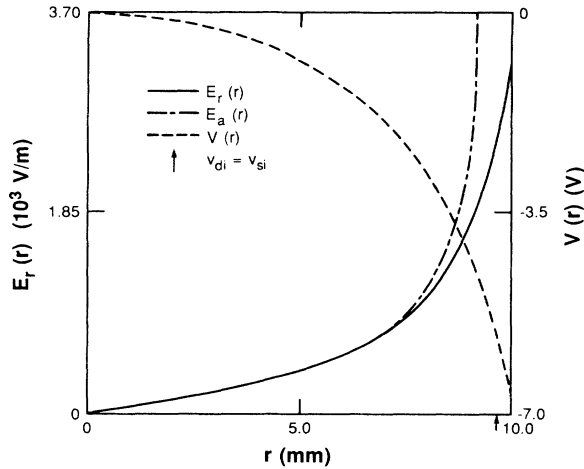
FIG. 2. Numerical calculations of the radial distributions for the electric field strength $E_r(r)$ and the resulting electric potential $V(r)$ for the parameters given in Fig. 1 (i.e., $p_0 R = 5.0$ Torr cm). The ambipolar radial electric field $E_a(r)$ is also shown for comparison.

FIG. 4. Numerical calculations of the radial distributions for the ion density $n_i(r)$, the electron density $n_e(r)$, and the net charged-particle density $\Delta n(r)$ in a helium discharge with $p_0 = 1.0$ Torr and $R = 0.5$ cm ($p_0 R = 0.5$ Torr cm), implying $T_e = 45\,000$ K, and yielding $v_i = 6.67 \times 10^5$ s^{-1}.

Ewald.[2] Finally, the instability point discussed in Sec. II at which the radial ion drift velocity v_{di} is equal to the isothermal ion sound speed v_{si} is also shown in Fig. 1. This point is very near the wall under these discharge conditions.

The radial electric field $E_r(r)$ and the resulting electric potential $V(r)$ are shown in Fig. 2. For comparison, the ambipolar radial electric field $E_a(r)$ calculated from the ambipolar diffusion theory is also plotted in this figure. The value of $E_r(r)$ is relatively small near the axis, but increases to larger values near the wall. This is again indicative of the development of the plasma sheath near the wall. A comparison between $E_r(r)$ and $E_a(r)$ indicates that the two values are equal near the axis, but deviate from each other near the wall. This deviation is due to

the fact that the ambipolar theory does not model the sheath region, with $E_a(r) \to + \infty$ for $r \to R$. The curve of $V(r)$ also shows the smooth transition from the bulk plasma region near the axis to the sheath region near the wall. The resulting value of the potential at the wall relative to the axis is $V(r = R) = -6.6$ V. This value can be compared with the value V_a given by Eq. (22a) in Ref. 14 for the quasineutral inertia limited theory of the positive column. For the discharge parameters discussed here, $V_a = -9.5$ V. The discrepancy between these two values is a result of the assumptions of quasineutrality and inertia limited flow used in deriving the expression for V_a.

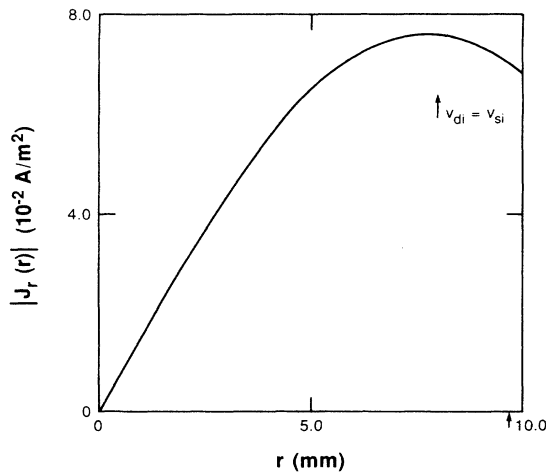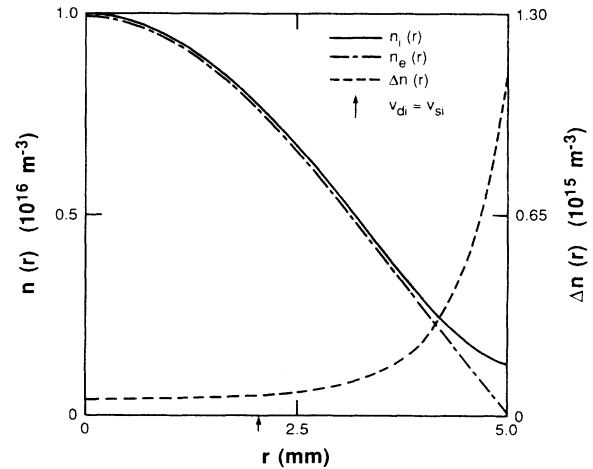Figure 3 is a plot of the magnitude of the radial

FIG. 3. Numerical calculations of the radial distribution for the magnitude of the charged-particle current density $|J_r(r)|$ for the parameters given in Fig. 1 (i.e., $p_0 R = 5.0$ Torr cm).
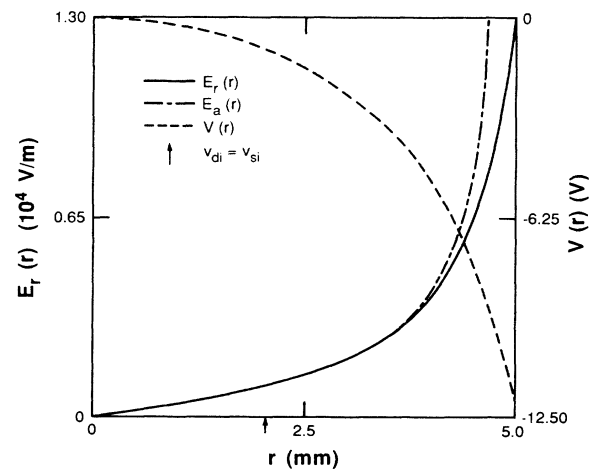

FIG. 5. Numerical calculations of the radial distributions for the electric field strength $E_r(r)$ and the resulting electric potential $V(r)$ for the parameters given in Fig. 4 (i.e., $p_0 R = 0.5$ Torr cm). The ambipolar radial electric field $E_a(r)$ is also shown for comparison.

charged-particle current density $|J_r(r)| = e\Gamma_r(r)$. The maximum in this curve is a consequence of the cylindrical geometry and the fact that the particle production rate $\nu_i n_e(r)$ decreases with increasing r. However, the total radial charged-particle current per unit length at radius r, $2\pi r|J_r(r)|$, is a monotonically increasing function of r, as required.

For comparison, the results of calculations for $p_0 = 1.0$ Torr and $R = 0.5$ cm are given in Figs. 4–6. This leads to a value $p_0 R = 0.5$ Torr cm, which is 10 times smaller than the value of $p_0 R$ for the previous case. For these conditions, the measurements of Leiby and Rogers imply $T_e = 45\,000$ K, leading to a required net charged-particle density on the axis of $\Delta n(r=0) = 4.9 \times 10^{13}$ m^{-3}. The resulting ionization frequency is $\nu_i = 6.67 \times 10^5$ s^{-1}. Figure 4 shows the plots of $n_i(r)$, $n_e(r)$, and $\Delta n(r)$ for this situation. As in the previous case, the curves for $n_i(r)$ and $n_e(r)$ are close to the shape of the zero-order Bessel function $J_0(2.4r/R)$ for the bulk of the plasma, with a significant deviation occurring, especially for $n_i(r)$, only near the tube wall. This deviation is again indicative of the development of a sheath region, as is also shown by the curve for $\Delta n(r)$. A comparison between Figs. 1 and 4 shows that the resulting sheath region is larger for smaller values of $p_0 R$. In addition, this comparison also shows that the values for $\Delta n(r)$ increase with decreasing $p_0 R$, with nearly an order of magnitude difference in $\Delta n(r)$ occurring between these two cases.

Figure 5 presents the results for $E_r(r)$ and $V(r)$ for this second case, along with the curve for $E_a(r)$ from the ambipolar diffusion theory. Again, the curve for $V(r)$ demonstrates the smooth transition from the bulk plasma region near the axis to the sheath region near the wall. For this situation, the resulting wall potential is $V(r=R) = -12.1$ V, as compared to the quasineutral inertia limited value $V_a = -16.5$ V. The magnitude of the

1.30

$V_{di} = V_{si}$

0.65

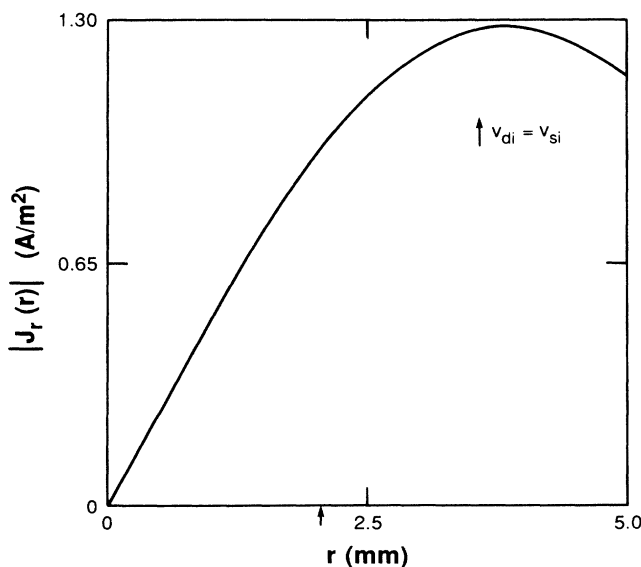$|J_r (r)|$ (A/m^2)

0

0   2.5   5.0

r (mm)

FIG. 6. Numerical calculations of the radial distribution for the magnitude of the charged-particle current density $|J_r(r)|$ for the parameters given in Fig. 4 (i.e., $p_0 R = 0.5$ Torr cm).

radial electric field shown in this figure is significantly larger than the electric field in Fig. 2. This is a consequence of the higher electron temperature for the situation depicted in Fig. 5, which leads to enhanced electron diffusion to the wall. This results in the generation of a larger space-charge-induced radial electric field in order to retard the electrons and accelerate the ions toward the wall. As a result, the point $v_{di} = v_{si}$ is closer to the axis in Fig. 5 than in Fig. 2, since the ion drift velocity at a given relative radial distance from the axis is larger for a larger electric field.

Figure 6 shows $|J_r(r)|$ for the situation where $p_0 R = 0.5$ Torr cm. The values of $|J_r(r)|$ for this case are more than an order of magnitude larger than those shown in Fig. 3.

From the above results, it is possible to investigate the applicability of the Bohm criterion, $v_{di} \geq (kT_e/m_i)^{1/2}$, for these discharge conditions.[15] For both discharge conditions discussed above, $v_{di}(r) < (kT_e/m_i)^{1/2}$ for all values of r. Thus the Bohm criterion is never met, even though the results presented in Figs. 1–6 clearly show the development of a sheath region near the discharge tube wall. The formation of a sheath region even in the absence of the Bohm criterion being fulfilled has been discussed previously by Ingold.[8]

The self-consistency of the theory in terms of the assumptions and boundary conditions used can be discussed in view of the calculations presented above. Assumption (4) in Sec. II states that ν_i is small with respect to ν_{mi} and ν_{me}. As can be seen by comparing the calculated values for ν_i with the values given for ν_{mi} and ν_{me}, this assumption is indeed satisfied for the cases presented. In addition to the boundary condition of Eq. (5) which was used in these calculations, another commonly used boundary condition is $n_e(r=R) = 0$. From Figs. 1 and 3 it is clear that this condition is closely approximated at $r = R$ in these figures. Indeed, calculations show that the tube radius would be increased by less than 0.2% if the boundary condition $n_e(r = R) = 0$ was used.

The two examples presented involve discharge conditions for which the radial diffusion of the charged particles is in the region of the ambipolar diffusion limit. However, the same equations can be used to calculate radial properties of the positive column when the radial charged-particle diffusion is in the transition region between the ambipolar diffusion limit and the free-diffusion limit.

IV. ORIGIN OF THE TOTAL RADIAL CHARGED-PARTICLE FLOW DENSITIES

As mentioned in Sec. I, several previous authors included Poisson's equation in the set of equations used when calculating the radial properties of the cylindrical positive column of a direct current discharge. However, they either omitted the charged-particle inertia term(s) or the ion diffusion term.[7,8] In comparison, the calculations presented in this paper were performed by including all terms of the conservation of momentum equations of the charged particles. The resulting total radial charged-particle current density has been discussed in the preced-

ing section. It is also interesting to investigate the relative importance of the three terms on the left-hand side of the conservation of momentum equations (2) and (3) on the total radial charged-particle flow density. The inertia terms represent the volume force needed to accelerate the existing and produced charged particles to their steady-state radial drift velocities. This force is supplied by the difference between the electric field, the diffusion, and the friction volume forces.

In order to compare the relative importance of the various terms on the total radial charged-particle flow density, Eqs. (2) and (3) can be rewritten as

$$\Gamma_r(r) = -\frac{1}{v_{mi}r}\frac{d}{dr}\left[\frac{r\Gamma_r^2(r)}{n_i(r)}\right] - \frac{kT_i}{m_i v_{mi}}\frac{d}{dr}n_i(r)$$
$$+ \frac{e}{m_i v_{mi}}n_i(r)E_r(r) , \qquad (6)$$

$$\Gamma_r(r) = -\frac{1}{v_{me}r}\frac{d}{dr}\left[\frac{r\Gamma_r^2(r)}{n_e(r)}\right] - \frac{kT_e}{m_e v_{me}}\frac{d}{dr}n_e(r)$$
$$- \frac{e}{m_e v_{me}}n_e(r)E_r(r) . \qquad (7)$$

Equation (6) gives the total radial ion flow density $\Gamma_r(r)$, which is equal to the total radial electron flow density given by Eq. (7). The first term on the right-hand side of Eqs. (6) and (7), the inertia flow density, does not represent a real flow density of the ions and electrons, re-

spectively. However, its relative magnitude with respect to the difference of the other two terms, i.e., the flow densities due to diffusion and the macroscopic electric field, will indicate the importance of the inclusion of the inertia terms in the calculations. In the following discussion, the three radial flow density terms for the ions will be represented by $\Gamma_{i_I}(r)$ for the inertial flow density, $\Gamma_{i_D}(r)$ for the diffusion flow density, and $\Gamma_{i_E}(r)$ for the electric field flow density. Similarly, $\Gamma_{e_I}(r)$, $\Gamma_{e_D}(r)$, and $\Gamma_{e_E}(r)$ will represent the three radial flow density terms for the electrons.

The total radial flow density and its three components are given for the case $p_0 R = 5.0$ Torr cm in Figs. 7 and 8 for the positive ions and electrons, respectively. The data of Fig. 7 show that the total ion radial flow density, $\Gamma_r(r)$, is almost completely a consequence of the induced electric field. The absolute values of $\Gamma_{i_I}(r)$ and $\Gamma_{i_D}(r)$ are several orders of magnitude smaller than $\Gamma_r(r)$ except very close to the tube axis, where all the flow densities approach zero. The data given in Fig. 8 show that for the electrons the absolute values of $\Gamma_{e_D}(r)$ and $\Gamma_{e_E}(r)$ are large with respect to the total electron radial flow density, $\Gamma_r(r)$. Moreover, the absolute value of $\Gamma_{e_I}(r)$ is several orders of magnitude smaller than $\Gamma_r(r)$. Therefore, for these discharge conditions, the radial electron density is approximately given by the Boltzmann distribution $n_e(r) = n_e(r=0)\exp[eV(r)/kT_e]$, as easily follows
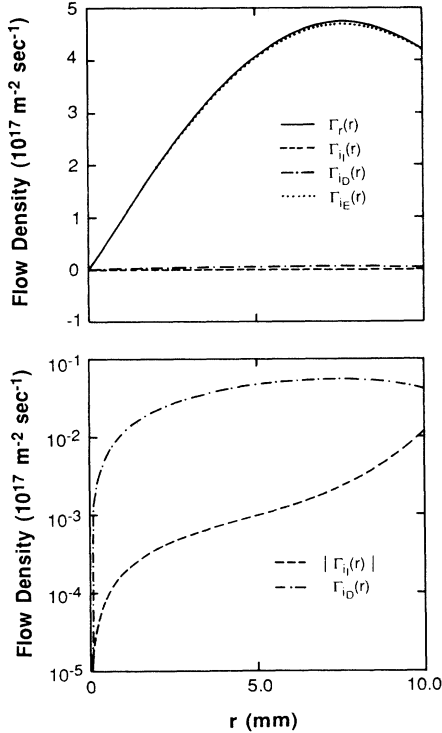

FIG. 7. Numerical calculations of the radial distributions for the positive ions of the total radial flow density $\Gamma_r(r)$, the inertia flow density $\Gamma_{i_I}(r)$, the diffusion flow density $\Gamma_{i_D}(r)$, and the electric field flow density $\Gamma_{i_E}(r)$. Data are for the parameters given in Fig. 1 (i.e., $p_0 R = 5.0$ Torr cm).
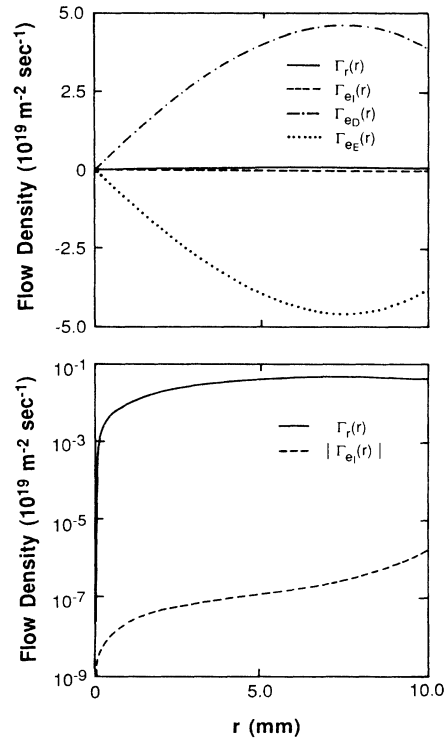

FIG. 8. Numerical calculations of the radial distributions for the electrons of the total radial flow density $\Gamma_r(r)$, the inertia flow density $\Gamma_{e_I}(r)$, the diffusion flow density $\Gamma_{e_D}(r)$, and the electric field flow density $\Gamma_{e_E}(r)$. Data are for the parameters given in Fig. 1 (i.e., $p_0 R = 5.0$ Torr cm).
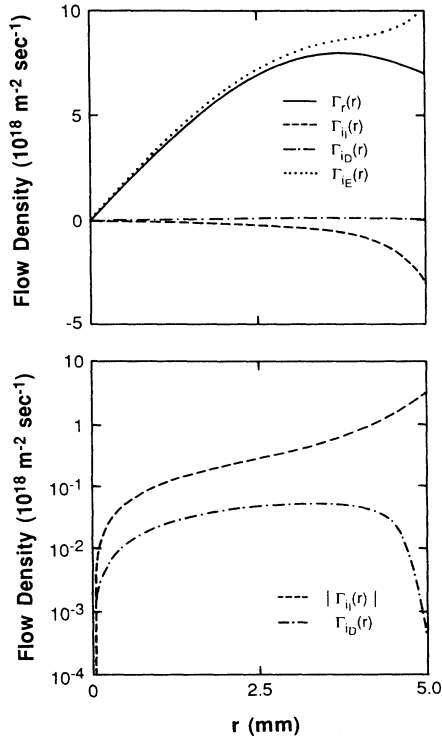
FIG. 9. Numerical calculations of the radial distributions for the positive ions of the total radial flow density $\Gamma_r(r)$, the inertia flow density $\Gamma_{i_I}(r)$, the diffusion flow density $\Gamma_{i_D}(r)$, and the electric field flow density $\Gamma_{i_E}(r)$. Data are for the parameters given in Fig. 4 (i.e., $p_0R = 0.5$ Torr cm).

FIG. 10. Numerical calculations of the radial distributions for the electrons of the total radial flow density $\Gamma_r(r)$, the inertia flow density $\Gamma_{e_I}(r)$, the diffusion flow density $\Gamma_{e_D}(r)$, and the electric field flow density $\Gamma_{e_E}(r)$. Data are for the parameters given in Fig. 4 (i.e., $p_0R = 0.5$ Torr cm).

from Eq. (7).

The flow densities for the case $p_0R = 0.5$ Torr cm are given in Figs. 9 and 10 for the ions and electrons, respectively. The data of Fig. 9 show that the absolute value of $\Gamma_{i_I}(r)$ is larger than 5% of the total ion flow density $\Gamma_r(r)$ over about half of the tube radius and reaches approximately 20% of the value of $\Gamma_r(r)$ close to the tube wall. The value of $\Gamma_{i_D}(r)$ is less than 1% of $\Gamma_r(r)$ for all values of the tube radius. The absolute values of $\Gamma_{e_D}(r)$ and $\Gamma_{e_E}(r)$ are again large with respect to the value of $\Gamma_r(r)$, as is shown in Fig. 10. However, the value of $\Gamma_{e_I}(r)$ increases strongly towards the tube wall and becomes more than 20% of the value of $\Gamma_r(r)$ close to the tube wall.

In summary, the calculations show that in a positive-column discharge produced in helium the diffusion flow density of positive ions, $\Gamma_{i_D}(r)$, is the only component of the total radial charged-particle flow density, $\Gamma_r(r)$, which is smaller than 1% for p_0R values varying from 0.5 to 5.0 Torr cm. For small p_0R values the inclusion of the inertia terms for both the positive ions, $\Gamma_{i_I}(r)$, and electrons, $\Gamma_{e_I}(r)$, has a non-negligible effect on the total radial charged-particle flow density. This implies, for this case, that the inertia forces should be included in the calculations and that the second and third terms on the right-hand side of Eqs. (6) and (7) cannot be interpreted
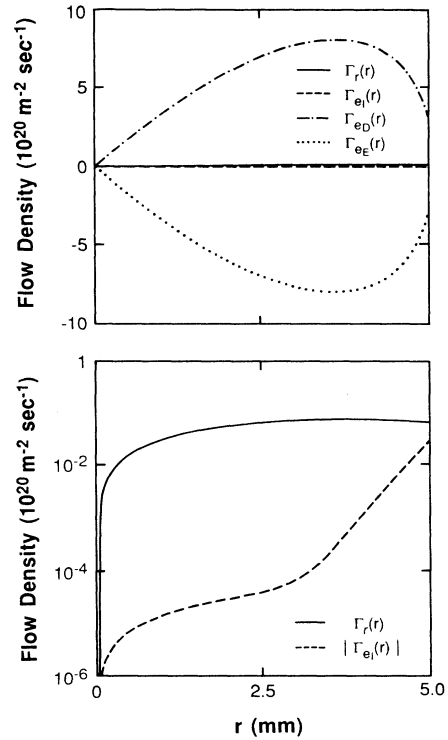
simply as the flow densities due to diffusion and induced electric field, respectively.

V. CONCLUSIONS

A model has been presented for the radial distribution of the ion and electron densities and electric field strength in the cylindrical positive column of a dc discharge for a plasma consisting of a singly charged positive-ion species, electrons, and neutral species. Under appropriate assumptions, the resulting set of equations involved consists of the particle-conservation equation, the momentum-conservation equations, and Poisson's equation. A method of solution for this set of equations using a power-series expansion has been outlined, which avoids the instability problem encountered by previous authors. This allows for the inclusion of all the volume force terms in the conservation of momentum equations for the ions and electrons.

The results of calculations based on this model show the development of the bulk plasma region near the discharge tube axis and the sheath region near the tube wall. There is no clear distinction between these two regions, with a smooth transition occurring from the bulk plasma region to the sheath region, as can be expected. While the results near the tube axis are consistent with the ambipolar model, they deviate considerably from this model in the sheath region near the wall. However, even

at the axis, there is a net space-charge density which in-
creases for decreasing values of $p_0 R$. The electric poten-
tial at the wall relative to the axis is on the order of the
value predicted by the quasineutral inertia limited theory,
with the wall potential increasing for decreasing values of
$p_0 R$. The results show that the development of a sheath
region can occur even for situations in which the Bohm
criterion is never met. The importance of the boundary
condition chosen for the electron density at the discharge
tube wall was investigated. It was found that the choice
of either Eq. (5) or $n_e(r = R) = 0$ as the boundary condi-
tion has little effect on the solution for the cases studied.

Finally, the relative importance of the three terms on
the left-hand side of the conservation of momentum equa-
tions (2) and (3) on the total radial charged-particle flow
density has been discussed. It was found that for $p_0 R$
values varying from 0.5 to 5.0 Torr cm the ion flow densi-
ty due to diffusion is less than 1% of the total ion radial
flow density. However, the effect of the inertia terms for
the ions and electrons on the total ion and electron radial
flow densities is non-negligible for small values of $p_0 R$.

ACKNOWLEDGMENTS

*Present address: Honeywell Systems and Research Center,
  3660 Technology Drive, Minneapolis, MN 55418.
[1]W. Schottky, Z. Phys. 25, 625 (1924).
[2]S. A. Self and H. N. Ewald, Phys. Fluids 9, 2486 (1966).
[3]H. W. Friedman, Phys. Fluids 10, 2053 (1967).
[4]W. P. Allis and D. J. Rose, Phys. Rev. 93, 84 (1954).
[5]I. M. Cohen, Phys. Fluids 6, 1492 (1963).
[6]I. M. Cohen and M. D. Kruskal, Phys. Fluids 8, 920 (1965).
[7]J. R. Forrest and R. N. Franklin, J. Phys. D 1, 1357 (1968).
[8]J. H. Ingold, Phys. Fluids 15, 75 (1972).

[9]H. W. Friedman and E. Levi, Phys. Fluids 10, 1499 (1967).
[10]H. B. Valentini, J. Phys. D 21, 311 (1988).
[11]J. H. Ingold and H. J. Oskam, Phys. Fluids 27, 214 (1984).
[12]C. C. Leiby, Jr., and C. W. Rogers (unpublished).
[13]H. J. Oskam, Philips Res. Rep. 13, 335 (1958).
[14]S. A. Self, Phys. Fluids 6, 1762 (1963).
[15]D. Bohm, in The Characteristics of Electrical Discharges in
  Magnetic Fields, edited by A. Guthrie and R. K. Wakerling
  (McGraw-Hill, New York, 1949), Chap. 3.